Julio A. Deiber[1]
Maria V. Piaggio[2]
Marta B. Peirotti[1]

[1]Instituto de Desarrollo Tecnológico para la Industria Química (INTEC), Universidad Nacional del Litoral (UNL), Consejo Nacional de Investigaciones Científicas y Técnicas (CONICET), Santa Fe, Argentina
[2]Cátedra de Bioquímica Básica de Macromoléculas, Facultad de Bioquímica y Ciencias Biológicas, UNL, Santa Fe, Argentina

Received August 16, 2013
Revised September 26, 2013
Accepted October 11, 2013

Research Article

Global chain properties of an all L-α-eicosapeptide with a secondary α-helix and its all retro D-inverso-α-eicosapeptide estimated through the modeling of their CZE-determined electrophoretic mobilities

Several global chain properties of relatively long peptides composed of 20 amino acid residues are estimated through the modeling of their experimental effective electrophoretic mobilities determined by CZE for $2 < pH < 6$. In this regard, an all L-α-eicosapeptide, including a secondary α-helix (Peptide 1) and its all retro D-inverso-α-eicosapeptide (Peptide 2), are considered. Despite Peptides 1 and 2 are isomeric chains, they do not present similar global conformations in the whole range of pH studied. These peptides may also differ in the quality of BGE components chain interactions depending on the pH value. Three Peptide 1 fragments (Peptides 3, 4, and 5) are also analyzed in this framework with the following purposes: (i) visualization of the effects of initial and final strands at each side of the α-helix on the global chain conformations of Peptide 1 at different pHs and (ii) analysis of global chain conformations of Peptides 1 and 2, and Peptide 1 fragments in relation to their p*I* values. Also, the peptide maximum and minimum hydrations predicted by the model, compatible with experimental effective electrophoretic mobilities at different pHs, are quantified and discussed, and needs for further research concerning chain hydration are proposed. It is shown that CZE is a useful analytical tool for peptidomimetic designs and purposes.

Keywords:
L-α-Eicosapeptide / Peptide effective electrophoretic mobility / Peptide global chain properties / Peptidomimetic structure function / Retro-D-inverso-α-eicosapeptide
DOI 10.1002/elps.201300395

Additional supporting information may be found in the online version of this article at the publisher's web-site

1 Introduction

At present, CZE is a useful analytical tool, which together with spectroscopy methodologies, provides the characterization of peptides synthesized via structure–function strategies for peptidomimetic purposes [1–9]. In this regard, CZE is a rapid and reliable technique providing experimental effective electrophoretic mobility μ_p^{exp} of peptides and proteins at well-defined BGE properties such as temperature *T*, electrical permittivity ε, viscosity η_s, ionic strength *I*, and pH ([10–15] and citations therein). Apart from the high capability to separate peptides and proteins, CZE is able to provide valuable information concerning chain conformations, electrokinetic properties as well as the quality of BGE components chain interactions of proteins and peptides at different pHs through the appropriate modeling of their effective electrophoretic mobilities [16–35].

This work shows that CZE may be useful in the peptidomimetic framework, where for instance non-L-α-amino acids are typically introduced into the natural L-α-peptide amino acid sequence (AAS). In these regards, developments of peptide hormones, peptide neurotransmitters, antimicrobial peptides, peptide inhibitor of HIV-1, peptide inhibitor of β-amyloid oligomerization, and peptide subunit vaccinate have been proposed, for instance as described in [1–6].

Correspondence: Dr. Julio A. Deiber, Instituto de Desarrollo Tecnológico para la Industria Química (INTEC), Universidad Nacional del Litoral (UNL), Consejo Nacional de Investigaciones Científicas y Técnicas (CONICET), Güemes 3450, 3000, Santa Fe, Argentina
E-mail: treoflu@santafe-conicet.gov.ar
Fax: +54-0-342-4550944

Abbreviations: **AAS**, amino acid sequence; **CG**, collapsed globule; **HC**, hybrid chain; **HZ**, hybrid zone; **PE**, polyelectrolyte; **RC**, random coil

In fact, many works demonstrated that incorporation of D-α-amino acids in the target peptide AAS has enhanced its affinity as ligand of biological receptors and also increased its resistance to proteolysis degradation [5, 7]. A wide range of case studies with favorable results were found and also some exceptions were reported confronting this strategy, mainly when the parent L-peptide adopted α-helical conformation in the bound state [8, 9]. Although we have no intention to enter into more details on this aspect of the subject, it is clear that the developments of drugs able to mimic natural L-α-peptides are invoking relevant isomerization properties associated with the corresponding retro-D-α-peptide, D-enantiomer (inverso peptide), and retropeptide isomers. These considerations may be even more complex when the parent L-α-peptide is large enough to show a tendency to form a secondary structure, such as the case study reported in [1] involving Peptides 1 and 2, where an α-helix is observed at pH 2.3 (see also Section 2.1). Within this brief context, this work has the purpose to estimate global chain properties at different pHs of the following peptides studied in [1] (see also Supporting Information Table 1): (i) the all L-α-eicosapeptide DDALYDDKNWDRAPQRCYYQ forming a secondary α-helix from 6th to 13th amino acid residues (designated Peptide 1), (ii) the corresponding all retro-D-inverso-α-eicosapeptide QYYCRQPARWNKDDYLADD of Peptide 1 (designated Peptide 2), (iii) the fragment of Peptide 1 where the last Y is missing (designated Peptide 3), (iv) the fragment of Peptide 1 where the terminal strand RCYYQ is absent (designated Peptide 4), and (v) the fragment of Peptide 1 where the initial strand DDALY is absent (designated Peptide 5). Peptide 1 is within the group of immunogenic peptides that react with the coat protein of human immunodeficiency virus HIV-1 gp120 in biochemical assays [1, 36–38]. The proposal is carried out on the base of our previous works concerning the modeling of μ_p^{exp} of peptides and proteins [19, 21, 22, 24, 26, 27, 29, 31–35].

This paper is organized as follows. Section 2.1 presents the data-processing procedures of experimental effective electrophoretic mobilities of peptides reported in [1] and studied here. Section 2.2 describes briefly both the electrophoretic mobility model used and the associated theoretical background, in addition to Supporting Information, to analyze then the resulting global properties of Peptides 1–5. In this section, physical concepts are presented to the extent they are able to apply to polyampholyte–polypeptide chains in general, to allow then the introduction of appropriate chain structural considerations that make clear distinctions between peptides and proteins. One important new concept described in this work is that different conformational substates may exist within basic chain conformational regimes already described in [29, 31]. This result is then effectively validated though the experimental and theoretical analyses of Peptides 1 and 2. In fact, Section 3 presents and discusses the main conformational differences between these peptides by taking into account that they have most of their electrokinetic properties quite similar. Concluding remarks and proposals for further research are provided in Section 4.

2 Materials and methods

2.1 Data processing of peptide experimental effective electrophoretic mobilities

Peptides 1 and 2 have the same number of amino acid residues $N = 20$ in the AAS (Supporting Information Table 1). Their average hydrophobicity index evaluated through the method used in [35] are reported in Supporting Information Table 1 indicating they have a moderate hydrophilic nature. Their μ_p^{exp} values at $I = 10$ mM and 25°C within the range $2 < \text{pH} < 6$ are taken directly from the fitted curves provided in [1]. Supporting Information Table 1 shows that the pI estimations corresponding to the null value $\mu_p^{exp} = 0$ obtained from either model calculations or experimental data fitting curves are quite close. Here data from the curve μ_p^{exp} versus pH in a range around the pI are avoided as a consequence of the rather low peptide effective charge number Z obtained. This result is more evident when the charge regulation phenomenon is considered, which moves the near molecule pH, designated pH*, closer to the pI value, thus differing from the protocol or bulk pH [19, 33]). In fact, Z is clearly lower than the titration or wild effective charge number Z_w, and $Z = Z_w = 0$ at pH = pI only. With these considerations, one avoids experimental errors associated with μ_p^{exp} for pH values approaching the pI (see also Section 3). Here, the effective charge $Z = Z_+ - |Z_-|$ is calculated from the positive Z_+ and negative Z_- charge numbers in the chain, respectively, using $\text{pH}^* = \text{pH} + e^2 Z/\{4\pi\varepsilon a_H(1 + \kappa a_H)\ln(10)k_B T\}$ [19, 21, 22, 24, 35]. Also emphasis is given on the fact that the charge regulation phenomenon is suppressed at the pI where pH* = pH = pI. In these expressions, e is the elementary charge, k_B is Boltzmann constant, a_H is the equivalent Stokes hydrodynamic radius as defined in [21, 26, 29], N_A is Avogadro constant, and $\kappa = (2e^2 I N_A 10^3/\varepsilon k_B T)^{1/2}$ is the Debye–Hückel parameter. In the calculation of pH*, the effect of small charge perturbations coming from electrostatic interactions among ionizing groups are neglected due to the difficulty in estimating average relative distances among them (see discussion on this aspect in [21, 26, 29]).

From the phenomenological point of view, Peptides 1 and 2 present different effective electrophoretic mobilities in the low range of pH (mainly below p$I \approx 4.27$) despite they are isomeric chains, while for pH > pI their mobilities tend to converge [1]. These experimental results clearly indicate the high sensitivity of CZE methods to detect different structural characteristics between a natural L-α-peptide and its retroinverso isomer in the framework of molecular mimicry. In addition from [1, 37], it was clear that both Peptides 1 and 2 included a secondary α-helix structure at pH 2.3 in several solvents and aqueous BGE. These results were demonstrated through NMR and circular dichroism spectroscopy methods. Therefore, these works are providing a challenging problem, which basically consists in the need to explain these experimental findings from the structural point of view of peptide chains, for instance through the modeling of their electrophoretic mobility to infer then peptide global properties [1, 25].

2.2 Theoretical model and definitions applied to Peptides 1–5

For the present analysis, peptides are characterized through the model described in our previous works, mainly in [19, 24, 26, 27, 29, 31]. Supporting Information provides a summary of the model used and a list of symbols with the corresponding units. Here, the integration of physical concepts and definitions associated with peptide conformations are presented. In this regard, the electrophoretic mobility of many peptides and proteins may be described along the Hückel branch of Henry theory valid for relatively small hydrodynamic particles with rather low electrical charge [32,35]. Thus, ion polarization relaxation is negligible [29] as long as $(e\zeta/k_BT) < 5/2$ and $\kappa a_H < 3$, for 1–1 symmetric BGEs. Here ζ is the particle zeta (electrokinetic) potential [35]. The model input data include, for instance, BGE properties, peptide AAS, and μ_p^{exp}, and then the model solution provides many output properties; mainly a_H, Z, and Ω. In fact, these peptides may have different shapes defined through the friction ratio $\Omega = f_o/f$ [21, 29], where Ω is evaluated in relation to the friction factor $f_o = 6\pi\eta_s a_H$ of the equivalent spherical model [27] and the actual friction $f = 6\pi\eta_s a_o N^{g_f}$ of the translating particle expressed through the hydrated chain fractal model [29, 31, 32, 35] involving the friction fractal dimension g_f (see expressions below and Supporting Information). Another possible phenomenon to be evaluated is the BGE slip at the peptide–particle surface when $\Omega > 1$ [35]. When the BGE does not slip at the particle surface, Ω is in addition designated asphericity [35], and spherical and aspherical particles yield $\Omega = 1$ and $\Omega \neq 1$, respectively. We found in general that $1/2 < \Omega < 3/2$ for peptides and proteins, depending mainly on AAS and protocol properties. Further it was recently shown that for $1 < \Omega < 3/2$, a partial or total BGE slip on the particle surface may exist [35] for spherical particles with slip length $b_{slip} = \eta_s/(\beta_{slip} + \eta_s/a_H)$, where β_{slip} is the slip coefficient.

Concerning the number of water molecules $H = 18\delta/M$ per chain, the actual hydrated particle volume must equal the equivalent sphere volume $4\pi a_H^3/3$. Here M refers to peptide molar mass and $\delta = \{(a_H/a_c)^3 - 1\}v_p/v_w$ (water mass/peptide mass) is the particle hydration, where a_c is the peptide compact radius (Supporting Information Table 1) defined in [21] and v_p and v_w are the chain- and water-specific volumes, respectively. A hydration function H in terms of peptide amino acid compositions and electrical charges of weak ionizing groups is necessary to correctly close the model. This function is composed of two parts as indicated in the expression for H provided in Supporting Information. One part evaluates the sum of hydrations of each amino acid residue on the AAS by considering their nonpolar, polar, and ionizing polar natures [24, 29], while the other part designated H_d considers the number of water molecules captured by the chain structure in certain conformational states. For instance, H_d may be positive for chain conformations occluding water and negative for rather closed conformations squeezing out water molecules residing around amino acid residues [27, 33–35]. In general, H_d was taken null mainly for proteins around their native states and for polypeptide chains with less than 50 amino acids residues [26, 29]. The appropriate values for H_d are dependent in part on protocol pH. An important physical aspect concerning chain hydration is that for a given μ_p^{exp} involving either peptides or proteins, $H_d = 0$ and $\Omega < 1$ implies the minimum δ value obtained from the model, while the same μ_p^{exp} with $H_d > 0$ and $\Omega = 1$ gives the maximum hydration value physically admissible for spherical particles. These results have been validated previously [21, 22, 27, 35]. Conversely, when a given μ_p^{exp} yields $\Omega > 1$ with $H_d = 0$ for both spherical and aspherical particles (BGE slip or stick at these particle surfaces may apply, respectively [35]) $H_d < 0$ is required to obtain $\Omega = 1$ thus giving a minimum hydration as long $a_H \geq a_c$ is satisfied [21, 35]. Some peptides assumed as spherical particles cannot give a solution in this last case because unphysical results are obtained when $a_H < a_c$ [21]. At present, our preliminary results indicate that a physical state of hydration between minimum and maximum values allowed by the model may exist on the basis of adding a thermodynamic constraint associated with the minimized electrical free energy of the charged chain (see also analyses in [22, 39]).

In this framework, the peptide AAS is considered as a chain of beads with a number average radius a_0 [26,27,29,31,32] calculated from van der Waals radii of amino acid residues [33–35] (see also [25, 28, 30] for a more general approach). This chain of beads allows one to evaluate global chain properties, electrokinetic chain states, and the associated global conformational regimes of peptides with the data output of the model. Therefore the electrical state of peptides is described through Z, Z_+, Z_-, and the total charge number $Z_T = Z_+ + |Z_-|$ is calculated at pH* (see [19, 26, 29, 35] and Supporting Information). The resulting chain packing fractal dimension $g_p = \log N/\log(a_H/a_o) \leq 3$ [27] indicates that for $g_p = 3$, the peptide has the compact volume $4\pi a_c^3/3$ with $a_H = a_c$ and $\delta = 0$. In general, g_p is associated with linear, plane, and spatial distributions of amino acid residues of the chain when this parameter increases [27]. In addition, a polyampholyte chain may be in the random coil (RC) regime when the effective $\Delta\sigma = |Z|/N$ and total $\sigma = Z_T/N$ charge number fractions are low enough to find this chain around Gaussian conformations [29, 31]. Under this physical situation, chain entropy tends to keep the string of beads in a disordered state, and from the basic theory of neutral polymers, the estimation of the RC chain gyration radius is $R_g \propto LC_N^{(1-g_f)} N^{g_f}$ [32], where the Flory-theta condition is obtained for $g_f = 1/2$ belonging to the unperturbed chain state. Here C_N is the Flory-characteristic ratio associated with local chain flexibility of a few interconnected bonds (short range intramolecular interactions) each one of length $L \approx 3.8$ Å (distance between two consecutive C_α in the backbone chain designated virtual peptide bond). Further, g_f quantifies the quality of BGE components chain interactions [31, 32] giving $1/3 < g_f < 1$ (large range intramolecular interactions are involved). For $g_f < 1/2$, poor BGE components chain interactions are obtained and a fully collapsed and perhaps

insoluble chain at $g_f \approx 1/3$ is generated, mainly for pH $\approx$ pI. On the other hand, for $g_f > 1/2$, good BGE components chain interactions yield a rather "unlocked chain structure" including self-avoiding random strands at $g_f \approx 3/5$. Since these equations describe the basic conformational states of the RC regime for quite low effective and total charge number fractions, other conformational regimes may exist as a consequence of chain destabilization due to electrostatic interaction effects. Typically, one finds the polyelectrolyte (PE), hybrid chain (HC) and collapsed globule (CG) regimes as described in [29]. In fact, in most of our previous results, mainly for proteins (high N) [27, 31], g_f values obtained were the "expected ones" according to different conformational regimes found by these chains as pH changed. Next, we will observe that this aspect is not necessarily and generally valid for peptides, where the number of amino acids residues is relatively lower. It is then clear that g_f values are indicating the type of "substates" at which a polyampholyte chain may exist within a given conformational regime, as discussed and illustrated in Section 3. It is also observed that combining Ω and f yields $g_f = 1/g_p - \log\Omega/\log N$, and for $\Omega \approx 1$ the friction fractal dimension is the inverse value of the packing fractal dimension, $g_f = 1/g_p$ [26, 29]. In this context, it is clear that approximate critical values of $\Delta\sigma$ and σ must be provided to establish when the RC regime becomes destabilized evolving to different conformational regimes due to the effect of intrachain electrostatic interactions. The scaling laws of critical $\Delta\sigma$ and σ were described in [40] and citations therein for $g_f = 1/2$ (the Flory-theta condition). More recently, these results were renormalized for $g_f \neq 1/2$ in [29]. Thus, two basic states for destabilization of a polyampholyte RC are found. One is the CG regime applicable for $\sigma > 1/uN^{(1-g_f)}$ due to the fluctuation-induced electrostatic attractions among pairs of opposing charges, and the other is the PE regime applying for $\Delta\sigma > 1/\sqrt{u}N^{(1-g_f/2)}$ due to the overall Coulombic repulsion between either positive or negative effective charge numbers. Parameter $u = l_B/L$ compares Bjerrum length $l_B = e^2/4\pi\varepsilon k_B T$ with the characteristic bond length L [29]. Here, changes in ε due to hydration effects are neglected (see details in [27, 29, 31]). Interesting is, in particular, the existence of transitions from either PE or CG regimens to the HC regime where chain hybrid zones (HZs) appear interconnected by chain strings [29, 40]. These HZs have been associated with the nucleation and formation of secondary structures when polyampholyte hetero chains of amino acid residues were considered, such as proteins and large peptides [29, 31]. The HC regime is found for $\sqrt{\sigma/N} < \Delta\sigma < u^x\sigma^y$ and $\sigma > 1/uN^{(1-g_f)}$, with $x = 1/2(1-g_f)$ and $y = (1-g_f/2)/(1-g_f)$ (see Fig. 1 in [29, 31]). In this regard, by taking into account the number of amino acid residues per chain blob being around $(u\sigma)^{-2}$ [40] and the relatively high values of $u = l_B/L$ found for peptides and proteins ($u \approx$ 2–6 depending on electrical permittivity within chain domain [29]), the blob size is close to the characteristic chain length L for typical total charge fractions of these analytes. This specific result for natural polypeptides is important for visualizing HZs as partial chain conformations with a tendency to form secondary structures involving direct interactions of several amino acid residues and also clusters of them near the HC–CG transition [29, 31].

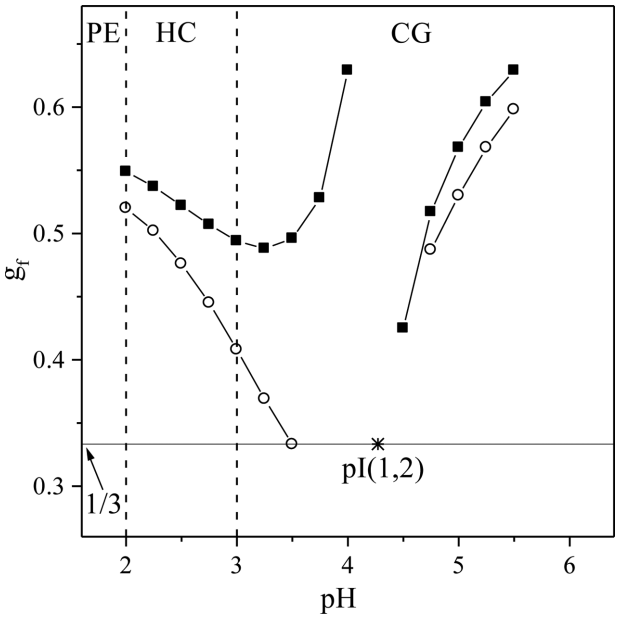

Figure 1. Friction fractal dimension g_f as a function of pH. Symbols (■) and (○) refer to Peptides 1 and 2, respectively, modeled as aspherical particles. Symbol (*) indicates pI = 4.27 for both peptides. Peptide code numbers are reported between parentheses. Dashed lines show approximate transitions from one conformational regime to another one. Also, PE, HC and CG refer to polyelectrolyte, hybrid chain and collapsed globule regimes, respectively.

Before analyzing the peptides under study here, it is important to point out that the experimental protocol used to obtain μ_p^{exp} has a BGE with a low ionic strength [1] and hence screening effects of electrostatic forces may be neglected [29].

3 Results and discussion

We found that model results of Peptide 3 were almost the same as those of Peptide 1. In fact, μ_p^{exp} values of these peptides [1] were not significantly at variance because their AAS differed in one Y residue only. Therefore, Peptide 3 is not analyzed further here. Supporting Information Tables 2–9 present numerical results of main global, electrokinetic, and hydrodynamic properties of Peptides 1, 2, 4, and 5 as obtained from the modeling of their μ_p^{exp} at different pH values. One conclusion concerning numerical results reported in these tables was that μ_p^{exp} values discarded around the pI in Section 2.1 were systematically yielding g_f and Ω out of physical ranges allowed by the theoretical framework described through $1/3 \leq g_f \leq 1$ and $H_d = 0$ with $1/2 < \Omega < 3/2$, or $H_d \neq 0$, $a_H \geq a_c$ with $\Omega = 1$ (see definitions in Sections 2.1 and 2.2). In these regards, the estimation of global chain properties defined in the theoretical model requires the experimentally determined electrophoretic mobilities measured by CZE

at well-defined conditions (pH, ionic strength, viscosity, and temperature of the BGE).

3.1 Aspherical particle model

Supporting Information Tables 2 and 3 show that Peptides 1 and 2 present the same electrokinetic properties (Z, Z_T, pH*, $\Delta\sigma$, and σ) when the model uses aspherical particles ($H_d = 0$ and $\Omega < 1$ giving minimum hydration, or $\Omega > 1$ for maximum hydration). Furthermore, the same hydration (δ or H), Stokes hydrodynamic radius (a_H), and consequently packing fractal dimension (g_p) are found due to the dependence of these last properties with the effective and total charge numbers (Supporting Information). These results are expected because Peptides 1 and 2 have the same amino acid residues. Nevertheless from these tables, the main differences between these two peptides are found in their friction ratios and hence friction fractal dimensions giving a clear distinction between peptide conformations through g_f values, remarkably for $3 <$ pH $<$ pI. In fact, Fig. 1 depicting g_f as a function of pH shows that within the range $2 <$ pH <3, both peptides are in the HC regime, where the formation of HZ and also the generation of a secondary structure are found. These results are consistent with NMR and circular dichroism experimental data reported in [37, 38] at around pH 2.3. In the HC regime, Peptide 1 has a g_f higher than Peptide 2 indicating that the friction coefficients of these particles are not necessarily equal (different qualities of their BGE components chain interactions) although their changes with pH follow quite similar pathways until around pH 3 where both peptides enter the CG regime. Then for pH > 3, Peptide 1 evolves by increasing g_f above 1/2 indicating conditions of good BGE components chain interactions and the formation of CG conformations with rather "unlocked" structures as the pH tends to the pI. Thus, Peptide 1 could be approaching the pI from the positive effective charge number side (Fig. 1) by keeping the secondary structure with the initial and terminal strands wrapping it to form the expected CG conformations. Although in the HC regime, calculations indicate that Peptides 1 and 2 have formed the α-helix expected, a different trend of g_f values of Peptide 2 from those of Peptide 1 for $3 <$ pH < 4.27 is observed clearly in Fig. 1. In fact, Peptide 2 presents a friction fractal dimension that evolves decreasing below $g_f \approx 1/2$ until $g_f \approx 1/3$ is reached at a pH still lower than the p$I = 4.27$. This result indicates that the BGE components chain interactions are very poor in this regime for Peptide 2 chain, which tends to get "rather insoluble" before the pH reaches the pI value. Here one would expect the absence of the α-helix formed previously in the HC regime for $2 <$ pH < 3, thus presenting quite strong CG conformations involving intrachain interactions and composed directly of disordered chain bonds. For pH $>$ pI, the conformational behaviors of both Peptides 1 and 2 are again quite similar, what is consistent with the fact that their electrophoretic mobilities start to converge within some experimental scattering errors as also noticed in [1].

Figure 2 illustrates Ω as a function of pH for Peptides 1 and 2. Here one visualizes that Peptide 2 may present partial or total slip between BGE and particle [35] where $\Omega > 1$ for $3 <$ pH < 4.27, as a consequence of the poor BGE components chain interactions already described in Fig. 1. The model provides $b_{slip} \approx 0.21$, 1.82, and 4.06 Å for pH 3, 3.25, and 3.5, respectively, indicating BGE partial slips satisfying consistently $b_{slip} < a_H$ [35]. From the discussion concerning Figs. 1 and 2, one infers that Peptides 1 and 2 differ substantially in their conformations within the positive effective charge number side approaching the pI, despite they are isomers. On the other hand for $2 <$ p H <3, they have similar HZs and perhaps secondary structures, but they do not have conformations necessarily equal due to differences in the qualities of their BGE components chain interactions found (Fig. 1 and Supporting Information Tables 2 and 3).

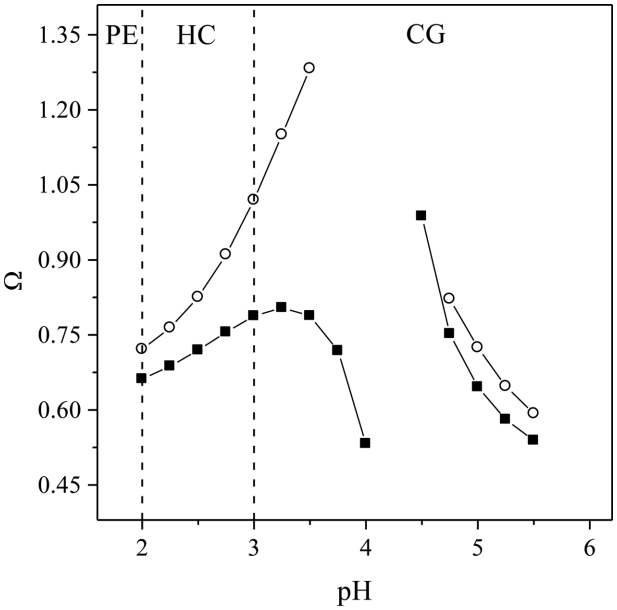

Figure 2. Friction ratio Ω as a function of pH. Symbols (■) and (○) refer to Peptides 1 and 2, respectively, modeled as aspherical particles. p$I = 4.27$ for both peptides. Dashed lines show approximate transitions from one conformational regime to another one. Also, PE, HC and CG refer to polyelectrolyte, hybrid chain and collapsed globule regimes, respectively.

Figure 3 and Supporting Information Tables 4 and 5 show that Peptides 4 and 5 (fragments of Peptide 1) have similar g_f evolutions with pH as that of the parent Peptide 1 in the HC regime for $2 <$ pH < 3, where the α-helix is expected to be formed. Thus, Peptides 4 and 5 tend to emulate the response of Peptide 1 for pH changes below pH 3. Furthermore for pH > 3, Peptide 4 follows the same trend as Peptide 1 due in part to their similar pI values (3.97 and 4.27, respectively) while Peptide 5 presents a plateau in a range a little above pH 3 as following Peptide 1 and 4 responses, but its higher pI around 6 is acting like an "attractor," perhaps first unwinding the α-helix and then collapsing at pI, where $g_f \approx 1/3$ involving very poor BGE components chain interactions. These results of Peptide 1 fragments indicate the functions played by the initial and terminal strings of the

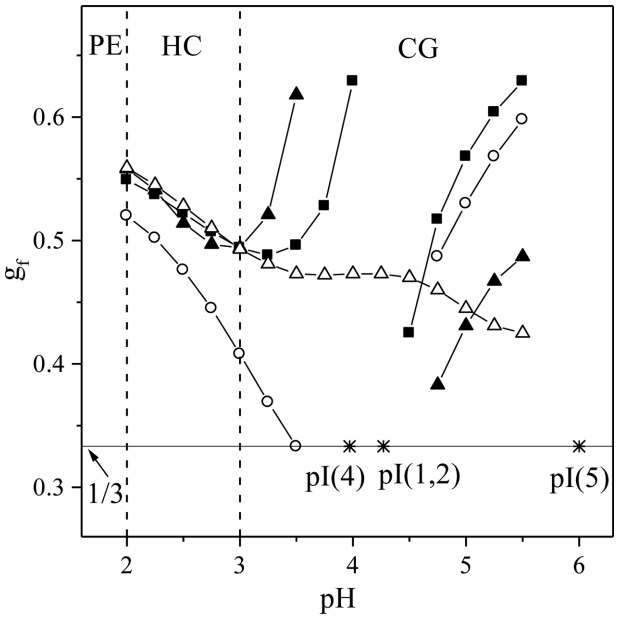

Figure 3. Friction fractal dimension g_f as a function of pH. Symbols (■), (○), (▲), and (Δ) refer to Peptides 1, 2, 4, and 5, respectively, modeled as aspherical particles. Symbol (*) refers to peptide p*I* values. Peptide code numbers are reported between parentheses. Dashed lines show approximate transitions from one conformational regime to another one. Also, PE, HC and CG refer to polyelectrolyte, hybrid chain and collapsed globule regimes, respectively.

parent peptide in order to control the appropriate p*I* value in peptidomimetic designs. Moreover, Peptides 1, 2, and 4, having almost equal p*I*, present a friction ratio tending to values greater than unity in Supporting Information Fig. 1, yielding a BGE slip on the particle [35] for pH values a little higher than their p*I*s. For instance, Peptide 4 presents $b_{slip} \approx 0.28$ and 1.94 Å for pH 4.75 and 5, respectively, indicating BGE partial slips satisfying consistently $b_{slip} < a_H$ [35]. These results also show that the conformation of Peptides 1, 2, and 4 achieved near their p*I* values from the negative effective charge number side is a strong CG similar to that obtained for Peptide 2 from positive effective charge number side. More generally this section showed that the all L-α-eicosapeptide and its all retro-D-inverso-α-eicosapeptide studied here could have similar conformations in the HC regime for $2 < pH < 3$ and also in a zone of the CG regime defined for $pH > pI$ where the collapsed secondary structure was not expected and rather good BGE components chain interactions prevail with $g_f \approx 3/5$ for pH 5–6. Relevant to this aspect is that the basic part of the titration curve depicted in Supporting Information Fig. 2 (a–g) cannot reach the HC regime at pH 6. This figure depicts a set of σ–Δσ plots to illustrate the pathway of Peptide 1 evolution, passing through different conformational regimes for the experimental range of pH values, validating the transitions reported in Figs. 1–3. In fact, we found from the model results that Peptides 1, 2, 4, and 5 had their PE–HC and HC–CG transitions for very similar values of pHs at around 2 and 3, respectively (Figs. 1–3 and Supporting Information Figs. 1, 3–6).

3.2 Spherical particle model

Supporting Information Tables 6 and 7 show that Peptides 1 and 2 present different electrokinetic properties (Z, Z_T, pH*, Δσ, and σ), particle hydration (δ or H), Stokes hydrodynamic radius (a_H), and consequently packing fractal dimension (g_p) when the model uses spherical particles ($\Omega = 1$ requiring $H_d > 0$ for maximum hydration or $H_d < 0$ for minimum hydration). Despite these differences in property values as a consequence of forcing the hydrated particle to have spherical shape, Supporting Information Tables 6 and 7 indicate that the main differences between the two peptides are again associated with g_f values. These results once more involve clear distinctions between Peptide 1 and 2 conformations mainly for $3 < pH < pI$. Nevertheless, for this case involving spherical particles the friction ratio is unity and $g_f = 1/g_p$. Consequently, different g_f and also g_p values are obtained due to a significant change of a_H from one peptide to another at each pH. Thus, Supporting Information Figs. 3 and 4 show a_H and g_f as a function of pH for Peptides 1 and 2. Concerning the change of a_H from one peptide to another at each pH, we found similar qualitative results as those reported in [1], where by assuming these peptides as spherical particles, the Stokes hydrodynamic radius of Peptide 1 was higher than that of Peptide 2. These results are consistent with the fact that the difference in μ_p^{exp} values depends inversely with Stokes hydrodynamic radii when the analytes are spherical particles with equal effective charges [19, 21, 22, 24, 26, 29, 31–35]. Nevertheless, the sizes of these particles in [1] are higher than those reported here in Supporting Information Table 8 due mainly to differences in the calculation of peptide effective charges. In fact, our model takes into account the charge regulation phenomenon.

Supporting Information Fig. 4 shows clear distinctions between Peptide 1 and 2 conformations through the g_f values mainly for $3 < pH < pI$. This figure also shows that within the range $2 < pH < 3$, both peptides are in the HC regime as described in Section 3.1. Supporting Information Figs. 5 and 6 and Supporting Information Tables 9 and 10 show that Peptides 4 and 5 have a similar g_f evolution with pH as that of the parent Peptide 1 in the HC regime for $2 < pH < 3$, where the α-helix is expected to be formed. In general, the same conclusions as those of Section 3.1 are obtained once more for $2 < pH < 6$.

Finally, peptide diffusivity $D = k_B T/\{6\pi\eta a_o N^{g_f}\}$ may be evaluated with g_f values obtained for both aspherical and spherical particles, as provided by the model at the running protocol conditions [29]. Thus, it was found that the diffusivities of Peptide 2 are greater than those of Peptide 1 in almost the whole experimental range of pH by a maximum factor of either 1.63 at pH 3.5 for aspherical particle and 1.37 at pH 3 for spherical particle. This aspect is also relevant in the peptidomimetic framework.

4 Concluding remarks

Peptides 1 and 2 differ substantially in their conformations within the CG regime for the positive effective charge number side approaching the p*I*, despite they are isomers. On the other hand for $2 < pH < 3$, they have similar HZs and hence secondary structure in the HC regime, although differences in the qualities of their BGE components chain interactions are evident. These results indicate the importance of the pH value at which the synthesized peptide for peptidomimetic purposes must satisfy the structure function strategy. It is also relevant to point out that the estimation of global chain properties evaluated in this work requires the experimentally determined electrophoretic mobilities measured by CZE at well-defined conditions (pH, ionic strength, viscosity, and temperature of the BGE).

From this study, it is clear that a definite state of peptide hydration between minimum and maximum values allowed by the model may exist. In this regard, further research should provide a thermodynamic constraint for the model, probably associated with the minimum electrical free energy of the peptide chain.

The authors wish to thank the financial aid received from Universidad Nacional del Litoral, Santa Fe, Argentina (CAI+D-2011) and CONICET (PIP-112–201101–00060).

The authors have declared no conflict of interest.

5 References

[1] Hearn, M. T. W., Keah, H. H., Boysen, R. I., Messana, I., Misiti, F., Rossetti, D. V., Giardina, B., Castagnola, M., *Anal. Chem.* 2000, *72*, 1964–1972.

[2] Wiley, R. A., Rich, D. H., *Med. Res. Rev.* 1993, *13*, 327–384.

[3] Fauchère, J. L., Thurieau, C., *Adv. Drug Res.* 1992, *23*, 127–159.

[4] Giannis, A., Kolter, T., *Angew. Chem. Int. Ed. Engl.* 1993, *32*, 1244–1267.

[5] Welch, B. D., VanDemark, A. P., Heroux, A., Hill, C. P., Kay, M. S., *PNAS* 2007, *104*, 16828–16833.

[6] Taylor, M., Moore, S., Mayes, J., Parkin, E., Beeg, M., Canovi, M., Gobbi, M., Mann, D. M. A., Allsop, D., *Biochemistry* 2010, *49*, 3261–3272.

[7] Sakurai, K., Chung, H. S., Kahne, D., *J. Am. Chem. Soc.* 2004, *126*, 16288–16289.

[8] Li, Ch., Pazgier, M., Li, J., Li, Ch., Liu, M., Zou, G., Li, Z., Chen, J., Tarasov, S. G., Lu, W-Y, Lu, W., *J. Biol. Chem.* 2010, *285*, 19572–19581.

[9] Li, Ch., Zhan, Ch., Zhao, L., Chen, X., Lu, W-Y, Lu, W., *Bioorg. Med. Chem.* 2013, *21*, 4045–4050.

[10] Dolník, V., *Electrophoresis* 2008, *29*, 143–156.

[11] El Rassi, Z., *Electrophoresis* 2010, *31*, 174–191.

[12] Kašička, V., *Electrophoresis* 2010, *31*, 122–146.

[13] Kašička, V., *Electrophoresis* 2012, *33*, 48–73.

[14] Selvaraju, S., El Rassi, Z., *Electrophoresis* 2012, *33*, 74–88.

[15] Righetti, P. G., Sebastiano, R., Citterio, A., *Proteomics* 2013, *13*, 325–340.

[16] Castagnola, M., Rossetti, D. V., Cassiano, L., Misiti, F., Pennacchietti, L., Giardina, B., Messana, I., *Electrophoresis* 1996, *17*, 1925–1930.

[17] Castagnola, M., Rossetti, D. V., Corda, M., Pellegrini, M., Misiti, F., Olianas, A., Giardina, B., Messana, I., *Electrophoresis* 1998, *19*, 2273–2277.

[18] Šolínová, V., Kašička, V., Koval, D., Hlaváček, J., *Electrophoresis* 2004, *25*, 2299–2308.

[19] Piaggio, M. V., Peirotti, M. B., Deiber, J. A., *Electrophoresis* 2005, *26*, 3232–3246.

[20] Xin, Y., Mitchell, H., Cameron, H., Allison, S. A., *J. Phys. Chem. B* 2006, *110*, 1038–1045.

[21] Piaggio, M. V., Peirotti, M. B., Deiber, J. A., *Electrophoresis* 2006, *27*, 4631–4647.

[22] Piaggio, M. V., Peirotti, M. B., Deiber, J. A., *Electrophoresis* 2007, *28*, 2223–2234.

[23] Šolínová, V., Kašička, V., Sázelová, P., Barth, T., Mikšík, I., *J. Chromatogr. A* 2007, *1155*, 146–153.

[24] Piaggio, M. V., Peirotti, M. B., Deiber, J. A., *Electrophoresis* 2007, *28*, 3658–3673.

[25] Pei, H., Xin, Y., Allison, S. A., *J. Sep. Sci.* 2008, *31*, 555–564.

[26] Peirotti, M. B., Piaggio, M. V., Deiber, J. A., *J. Sep. Sci.* 2008, *31*, 548–554.

[27] Piaggio, M. V., Peirotti, M. B., Deiber, J. A., *Electrophoresis* 2009, *30*, 2328–2336.

[28] Pei, H., Allison, S., *J. Chromatogr. A.* 2009, *1216*, 1908–1916.

[29] Piaggio, M. V., Peirotti, M. B., Deiber, J. A., *J. Sep. Sci.* 2010, *33*, 2423–2429.

[30] Allison, S. A., Pei, H., Allen, M., Brown, J., Chang-II, K., Zhen, Y., *J. Sep. Sci.* 2010, *33*, 2439–2446.

[31] Deiber, J. A., Piaggio, M. V., Peirotti, M. B., *Electrophoresis* 2011, *32*, 2779–2787.

[32] Deiber, J. A., Piaggio, M. V., Peirotti, M. B., *Electrophoresis* 2012, *33*, 990–999.

[33] Deiber, J. A., Piaggio, M. V., Peirotti, M. B., *Electrophoresis* 2013, *34*, 700–707.

[34] Deiber, J. A., Piaggio, M. V., Peirotti, M. B., *Electrophoresis* 2013, *34*, 708–715.

[35] Deiber, J. A., Piaggio, M. V., Peirotti, M. B., *Electrophoresis* 2013, *34*, 2648–2654.

[36] Sitaram, B. R., Keah, H. H., Hearn, M. T. W., *J. Chromatogr. A* 1999, *857*, 263–273.

[37] Higgins, K. A., Bicknell, W., Keah, H. H., Hearn, M. T. W., *J. Pept. Res.* 1997, *50*, 421–435.

[38] Keah, H. H., Kecorius, E., Hearn, M. T. W., *J. Pept. Res.* 1998, *51*, 2–8.

[39] Tanford, C., *Advan. Protein Chem.* 1970, *24*, 1–95.

[40] Dobrynin, A. V., Colby, R. H., Rubinstein, M., *J. Polym. Sci. Part B Polym. Phys.* 2004, *42*, 3513–3538.

